



# The Structure of Ga-Sb-Se Glasses by High-Resolution X-Ray Photoelectron Spectroscopy

Roman Golovchak, Laurent Calvez, Alicia Lecomte, Andriy Kovalskiy, Henry Luftman, Himanshu Jain

## ► To cite this version:

Roman Golovchak, Laurent Calvez, Alicia Lecomte, Andriy Kovalskiy, Henry Luftman, et al.. The Structure of Ga-Sb-Se Glasses by High-Resolution X-Ray Photoelectron Spectroscopy. *physica status solidi (b)*, 2021, 258 (6), pp.2100074. 10.1002/pssb.202100074 . hal-03217074

**HAL Id: hal-03217074**

**<https://hal.science/hal-03217074>**

Submitted on 5 May 2021

**HAL** is a multi-disciplinary open access archive for the deposit and dissemination of scientific research documents, whether they are published or not. The documents may come from teaching and research institutions in France or abroad, or from public or private research centers.

L'archive ouverte pluridisciplinaire **HAL**, est destinée au dépôt et à la diffusion de documents scientifiques de niveau recherche, publiés ou non, émanant des établissements d'enseignement et de recherche français ou étrangers, des laboratoires publics ou privés.

## The structure of Ga-Sb-Se glasses by high-resolution XPS

*Roman Golovchak\**, Laurent Calvez, Alicia Lecomte, Andriy Kovalskiy, Henry Luftman, Himanshu Jain

Prof. R. Golovchak, Prof. A. Kovalskiy  
Department of Physics, Engineering and Astronomy, Austin Peay State University,  
601 College St., Clarksville, TN 37044, USA  
E-mail: holovchakr@apsu.edu (R. Golovchak)

Dr. L. Calvez, A. Lecomte,  
University of Rennes-1, CNRS, ISCR (Institut des Sciences Chimiques de Rennes) - UMR 6226, F-35000 Rennes, France

Dr. H. Luftman, Prof. H. Jain  
Department of Materials Science and Engineering, Lehigh University, 5 East Packer Avenue,  
Bethlehem, PA 18015-3195, USA

Keywords: chalcogenide glass, electronic and atomic structure, XPS

To understand the unique physical properties of Ga-Sb-Se glasses, high-resolution XPS studies have been performed on representative compositions within the glass-forming region. The observed peaks in the valence band as well as in Ga, Sb and Se core level XPS spectra are related to the main structural building blocks of the covalent network. On the basis of disproportionality equations and quantitative XPS analysis, the Se-Se-Se fragments are shown to exist in the glasses with 65 and 68 at.% of Se, whereas the samples with lower Se content are shown to contain a significant concentration of Se-Se bonds instead. Although the majority of Ga atoms are deemed to form 4-fold coordinated units, the existence of Ga atoms in 3-fold coordination, those bonded to other metal as well as forming Ga clusters of undissolved Ga are also plausible on the basis of Ga 3d XPS spectrum analysis. Partial or full destruction of antimony selenide pyramids is found in glasses with low Se content.

This article has been accepted for publication and undergone full peer review but has not been through the copyediting, typesetting, pagination and proofreading process, which may lead to differences between this version and the [Version of Record](#). Please cite this article as [doi: 10.1002/pssb.202100074](https://doi.org/10.1002/pssb.202100074).

## 1. Introduction

Antimony selenide glasses possess interesting and unique electronic, thermo/photoelectric and optical properties,<sup>[1-9]</sup> which can lead to many applications in photonics and electronics. However, the use of binary Sb-Se glasses suffers from their high tendency to crystallization. The stoichiometric antimony triselenide  $\text{Sb}_{40}\text{Se}_{60}$  (or  $\text{Sb}_2\text{Se}_3$ ), for example, easily crystallizes even during melt-quenching procedure normally used to synthesize chalcogenide glasses.<sup>[10]</sup> To avoid crystallization, a third chemical element such as As or Ge is usually introduced into the composition and, therefore, corresponding glasses within Ge-Sb-Se or Sb-As-Se families are widely investigated.<sup>[10-12]</sup> Recently it was discovered, that incorporation of Ga also significantly improves the glass-forming ability of antimony selenides.<sup>[13]</sup> Although the unique properties of Ga-Sb-Se thin films (like the low-power phase-change memory effect) have been noticed earlier,<sup>[14]</sup> the possibility to have a bulk glass opens another broad range of applications in photonics. Besides the inherent high transparency in IR region of spectrum, which makes them suitable for IR fibers and sensor applications, the presence of Ga in their structure should also lead to better solubility of rare-earth elements.<sup>[15]</sup> Because of this, the rare-earth doped Ga-Sb-Se glasses would be very attractive for applications in up and down energy conversion devices, lasers, bright sources and optical amplifiers in the mid-IR optical range.<sup>[16]</sup>

Nevertheless, the structural development within Ga-Sb-Se glass-forming system as well as the role of each chemical element in glass formation remain poorly investigated. The main focus of this research is to understand the short-range order structure around constituting chemical elements and its evolution with composition. Specifically, it would be of practical interest to identify if Ga behaves similarly to trivalent (like As or Sb) or tetravalent (like Ge or Si) chemical elements. High-resolution X-ray photoelectron spectroscopy (XPS) is an appropriate tool for this purpose, successfully applied previously to explain structural development in many binary and ternary glasses (e.g. As-Se, Ge-Se, As-S, Ge-S, As-Ge-Se, Ga-Ge-Se, Ge-Sb-Se and Ga-Ge-Sb-S).<sup>[17-24]</sup> It

allows not only to identify the main building blocks at the short-range order of glass networks, but also to quantify their moieties.

## 2. Experimental

The  $\text{Ga}_4\text{Sb}_{31}\text{Se}_{65}$ ,  $\text{Ga}_8\text{Sb}_{24}\text{Se}_{68}$ ,  $\text{Ga}_8\text{Sb}_{27}\text{Se}_{65}$ ,  $\text{Ga}_8\text{Sb}_{37}\text{Se}_{55}$ ,  $\text{Ga}_8\text{Sb}_{40}\text{Se}_{52}$  and  $\text{Ga}_{12}\text{Sb}_{23}\text{Se}_{65}$  glasses covering the glass-forming region of interest were prepared by the conventional melt-quench method from a mixture of high-purity elemental gallium, antimony and selenium (99.999 % purity). The vacuum-sealed silica tube of 7 mm inner diameter with raw ingredients was maintained in a rocking furnace at 950 °C for 12 h and then quenched from 870 °C into iced water. The samples were annealed 10 °C below  $T_g$  for 5 h to relieve mechanical strains induced by rapid quenching. Vitreous state of the prepared materials was ascertained from XRD patterns and near-IR transmittance.

High resolution XPS spectra were recorded with a Scienta ESCA-300 spectrometer using monochromatic Al  $K_\alpha$  X-rays (1486.6 eV) under a vacuum of  $2 \times 10^{-8}$  Torr (or less), as described elsewhere.<sup>[17-24]</sup> To obtain structural information about the bulk of glass, the samples were fractured directly in the ultrahigh-vacuum chamber of the spectrometer and the data were collected from these freshly created surfaces. A low energy (<10 eV) electron flood gun was used to neutralize surface charging that resulted from the photoelectron emission. The experimental energy of XPS spectral features was adjusted according to the position of 1s core level peak (284.6 eV) of adventitious carbon and Se Auger lines.<sup>[25]</sup> XPS data were analyzed with standard CASA-XPS software package, using Shirley background and a pseudo-Voigt line shape for the core level peaks.<sup>[26]</sup> The pseudo-Voigt function was approximated by Gaussian/Lorentzian product form, where the mixing was fixed to be 0.3 (0 is a pure Gaussian, 1 is a pure Lorentzian) for all doublets of the analyzed core-levels. The 3d core-level XPS spectra of Ga, 4d core-level XPS spectra of Sb and 3d core-level XPS spectra of Se were used for quantitative analysis of short-range chemical order in the investigated glasses. These spectra were fitted by a number of doublets (which

consisted of  $d_{5/2}$  and  $d_{3/2}$  components owing to spin-orbit splitting), which depended on the improvements in goodness of the fit. Constraints used for the  $d_{5/2}$  and  $d_{3/2}$  components within a doublet were as follows: area ratio 1.45, same full width at half maximum (*fwhm*) and a peak separation of 0.46 eV for Ga, 1.24 eV for Sb, 0.85 eV for Se core levels. Different *fwhm* values were allowed for independent doublets of the same core-level peak. With these constraints, the uncertainties in the peak position (binding energy, *BE*) and area (*A*) of each component were  $\pm 0.05$  eV and  $\pm 2$  % respectively.

### 3. Results and discussion

There was no evidence of significant concentration of impurities (oxygen-based complexes being most likely) in the XPS survey spectra of the freshly fractured samples. Their compositions, estimated from the area ratios of main core level peaks of the constituent chemical elements and the reference spectra in PHI handbook,<sup>[25]</sup> were close to the nominal values (deviations were within  $\pm 1$  at.% error bar).

The recorded valence band XPS spectra (**Figure 1**) correlate well with the valence band spectra obtained earlier for bulk Ge-Sb-Se and Ga-Ge-Se glasses.<sup>[22,23]</sup> The 4*p* lone pair electrons and 4*p* bonding states of Se contribute to the XPS signal at about 2 eV and 5 eV, respectively. The signal at  $\sim 2.0$  eV may also include intensity from Sb 5*p* bonding electrons participating in the formation of Sb-Sb bonds, as suggested previously.<sup>[27]</sup> The density-of-states maximum at  $\sim 3$  eV is due to the broadening of Se 4*p* bonding states peak by Se-Ga and Se-Sb bonds, as well as metal-metal bonding states.<sup>[22,23,25]</sup> Electronic density of states calculations performed for crystalline GaSe and Ga<sub>2</sub>Se<sub>3</sub> also support these assignments.<sup>[28]</sup> The broad features in the range 6-16 eV correspond to the overlapping signal from Ga 4*s*, Sb 5*s* and Se 4*s* electrons.<sup>[17,18,22,23,29,30]</sup>

The analysis of chemical order around constituent chemical elements can be accomplished through the quantification of corresponding core-level XPS spectra, taking into account that chemical shifts in the XPS peaks depend on the electron density distribution around probed

element, which is determined mainly by electronegativity of neighbors, their electronic configuration and charge state. Within such approach, each separate doublet appearing in the fit of the experimental XPS core level spectrum would correspond to a specific chemical environment (structural fragment) of the probed element and its electronic configuration. So, the number of doublets in the fit gives the number of possible chemical environments for the absorbing atom, whereas the area under each doublet gives the concentration of the associated moiety. The identification of regular structural fragments through their chemical shifts is based on our previous XPS studies in binary and ternary Ga, Sb and Se-containing glasses.<sup>[17,18,22,23,29,30]</sup> The difference in electronegativity values of the constituent chemical elements ( $\chi_{Ga}=1.81$ ,  $\chi_{Sb}=2.05$ ,  $\chi_{Se}=2.55$ )<sup>[31]</sup> allows good resolution of the doublets corresponding to different chemical environments, assuming covalently bonded glass network.

As could be seen from the fitting of Se 3d core level XPS spectra (**Figure 2, Table 1**), all glasses with 65 and 68 at.% of Se contain Se-**Se**-Se fragments (absorbing atom is in bold font) in their structure, though, not exceeding 10 % of all Se sites. The *BE* of primary ( $d_{5/2}$ ) component of corresponding doublet at ~54.7 eV agrees well with *BE* of Se-**Se**-Se fragments observed in a number of Se-containing glasses.<sup>[17,18,21-23]</sup> The other well-resolved doublet with primary component at ~54.2 eV corresponds to Se-Se bridges according to our previous XPS analysis in Ga/Ge-containing selenides.<sup>[18,22,23]</sup> The above two Se-rich fragments were not expected in Se-poor compositions, where there is a deficit of Se atoms needed to satisfy the main valence of Ga and Sb. Their existence, therefore, indicates that metal-metal bonds are unavoidable in these materials. The Se-shared structural fragments (Sb-based units corner-shared with each other or with Ga-based tetrahedra) give rise to a doublet with primary component at ~53.6 eV (Table 1) in Se core level XPS spectrum, while Se between Ga atoms only is most probably responsible for a doublet with primary component at ~53.2 eV (Table 1). The latter assumption is based on a fact that electronegativity of Ga is the lowest and, therefore, the corresponding doublet should be observed on the most low-*BE* side. This, however, can be debated due to a fact that Ga is usually 4-fold

coordinated in chalcogenide matrix,<sup>[23,32,33]</sup> although with a negative effective charge. The above assignments for Se environment correlate well with <sup>77</sup>Se NMR studies and molecular dynamics simulations of Ga<sub>8</sub>Sb<sub>27</sub>Se<sub>65</sub> glass.<sup>[34]</sup>

The Ga 3*d* core level XPS spectra consist of a strong doublet with primary (*d*<sub>5/2</sub>) component at ~19.4 eV (**Figure 3, Table 2**), which corresponds to Ga coordinated with four Se atoms.<sup>[23,35]</sup> In addition, the low-*BE* doublet with primary component at ~18.8 eV can be resolved in Ga<sub>8</sub>Sb<sub>27</sub>Se<sub>65</sub> and Ga<sub>12</sub>Sb<sub>23</sub>Se<sub>65</sub> samples (Table 2). With varying probability it can be associated with 3-fold coordinated [GaSe<sub>3/2</sub>] units, Ga-metal-bonded units, or Ga clusters of undissolved Ga.

When Se content is high, as in Ga<sub>8</sub>Sb<sub>24</sub>Se<sub>68</sub> sample, all Sb atoms form [SbSe<sub>3/2</sub>] pyramids, which gives rise to the Sb 4*d* core level XPS peak with primary component (*d*<sub>5/2</sub>) at ~33.0 eV (**Figure 4, Table 3**). Owing to slightly higher *fwhm*, this peak might contain also doublets associated with Sb-based units of higher coordination as suggested in [Ref. 34], but they could not be unambiguously resolved by XPS in present studies. Decrease in Se content causes partial or full destruction of these units via the replacement of one or more Se atoms in [SbSe<sub>3/2</sub>] pyramids with metals (Sb or Ga).<sup>[22,36]</sup> This process gives rise to a doublet with primary components at ~32.6 eV if only one Se atom in pyramid is substituted. If two Se atoms are replaced with Sb or Ga, the core level further shifts to the low-*BE* region, leading to the doublet with primary component at ~32.1 eV. We believe the formation of metal clusters where all neighbors in [SbSe<sub>3/2</sub>] pyramid are replaced with Ga or Sb, is a reason of the observed doublet in Sb 4*d* core level XPS spectrum with primary component at ~31.8 eV (Table 3).

To verify that the above doublet assignments are reasonable, the fitting results are combined with disproportionality analysis, which assumes full saturation of covalent bonds in homogeneous glass network. Then, the 4-fold coordinated Ga atom removes 2 full Se atoms from the pool (each Ga atom is bonded to 4 Se atoms, which are half-shared with other structural units – so unit would be GaSe<sub>2</sub>); every 3-fold coordinated Sb atom removes 1.5 Se atoms (each Sb atom is bonded to 3 Se atoms, which are half-shared with other structural units – so unit would be SbSe<sub>1.5</sub>). Starting from

fully corner-shared tetrahedra/pyramids network (built of  $\text{GaSe}_2$  and  $\text{SbSe}_{1.5}$  units), we can determine the moieties of Se atoms involved in  $\text{GaSe}_2$  and  $\text{SbSe}_{1.5}$  units and redundant Se needed to satisfy the nominal composition. For example, in the case of  $\text{Ga}_8\text{Sb}_{24}\text{Se}_{68}$  composition one can write:

$$\text{Ga}_8\text{Sb}_{24}\text{Se}_{68} = x \cdot \text{GaSe}_2 + y \cdot \text{SbSe}_{1.5} + z \cdot \text{Se} \quad (1)$$

The XPS fitting results (Table 2 and 3) show that all Ga atoms form  $\text{GaSe}_2$  units and all Sb atoms form  $\text{SbSe}_{1.5}$  units (only one doublet is present in the respective core level fits with no indication of metal-metal bonds), which validates equation (1) and gives  $x = 8$  and  $y = 24$ . A simple calculation from (1) for a number of Se atoms gives  $z = 68 - 24 \cdot 1.5 - 8 \cdot 2 = 16$ . So, we have 16 redundant Se atoms which have to be inserted into the covalent network of corner-shared pyramids and tetrahedra to preserve the composition. If we insert a Se atom next to the Se shared between 2 metals (Ga or Sb), we produce 2 complexes  $\text{Sb}(\text{Ga})\text{-Se-Se}$  instead of one  $\text{Sb}(\text{Ga})\text{-Se-Sb}(\text{Ga})$ . However, if we insert the Se atom into the formed Se-Se bridge, the number of  $\text{Sb}(\text{Ga})\text{-Se-Se}$  complexes would not change, but additional  $\text{Se-Se-Se}$  complex would be created. According to XPS data in Table 1, there are 8 % out of 68 Se atoms participating in  $\text{Se-Se-Se}$  complexes (separate doublet in Se core level fit), which gives 5.44 of actual number of Se atoms (although fractions have no physical meaning, we keep them for the sake of accuracy). So,  $16 - 5.44 = 10.56$  of Se atoms must have been inserted into  $\text{Sb}(\text{Ga})\text{-Se-Sb}(\text{Ga})$  fragments, producing in total  $10.56 \cdot 2 = 21.12$  of Se atoms in  $\text{Sb}(\text{Ga})\text{-Se-Se}$  configurations. This number constitutes ~31% of all Se sites in nominal  $\text{Ga}_8\text{Sb}_{24}\text{Se}_{68}$  composition. The moiety of  $\text{Sb}(\text{Ga})\text{-Se-Se}$  complexes obtained from experimental XPS fit is ~32% (Table 1), which nicely correlates to the considered disproportionality equation (1). It should be emphasized here, that area under the doublet (which gives moiety of structural complex) was not restricted during the fit and, in principle, could differ from the moieties calculated according to (1).

Disproportionality equation for the  $\text{Ga}_8\text{Sb}_{40}\text{Se}_{52}$  composition



$$\text{Ga}_8\text{Sb}_{40}\text{Se}_{52} = x \cdot \text{GaSe}_2 + y \cdot \text{SbSe}_{1.5} + z \cdot \text{Se} \quad (2)$$

would give  $z < 0$ , meaning that it is impossible to have redundant Se atoms and, therefore, the **Se-Se** complexes. So, their absence in Se core level XPS fit (Table 1) is quite reasonable. Moreover, there are not enough Se atoms even to satisfy the neighbors of Sb and Ga (76 Se atoms are needed, while we have only 52) according to their main valences (stoichiometry). It means that we must have pyramids and/or tetrahedra, where one or more of Se atoms are substituted with metal (Ga or Sb). According to Table 2 we see that Ga satisfies its coordination with Se forming  $\text{GaSe}_2$  structural units only. Obviously, this should happen at the expense of  $\text{SbSe}_{1.5}$  pyramids. Taking into account also  $\sim 7\%$  of **Sb(Ga)-Se-Se** complexes as obtained from XPS fitting (Table 1), the disproportionality equation for  $\text{Ga}_8\text{Sb}_{40}\text{Se}_{52}$  composition should be written as

$$\text{Ga}_8\text{Sb}_{40}\text{Se}_{52} = 8 \cdot \text{GaSe}_2 + x \cdot \text{SbSe}_{1.5} + y \cdot \text{SbSe} + z \cdot \text{SbSe}_{0.5} + 1.82 \cdot \text{Se} \quad (3)$$

Further, we have obtained only 2 doublets in Sb 4*d* core level XPS spectrum fit (Table 3), which means that either  $x$ , or  $y$ , or  $z$  must be zero. To start with, let us assume that the first doublet with primary component at  $\sim 32.6$  eV is caused by  $\text{SbSe}_{1.5}$  pyramid (all neighbors are Se). Then  $x=24$  (60 % moiety out of 40 Sb atoms as obtained from the fit, Table 3), and we need  $24 \cdot 1.5 = 36$  Se atoms to satisfy this condition. On the other hand, the available Se atoms can be estimated from (3) as  $52 - 16 - 1.82 = 34.18$ , which is not enough, and we need also some Se atoms to form other 40% of SbSe-based units. Obviously, the first doublet cannot be associated with  $\text{SbSe}_{1.5}$  pyramids and  $x$  must be 0. Now, let us verify the possibility to assign the doublet with primary component at  $\sim 32.6$  eV to SbSe and the one at  $\sim 32.1$  eV to  $\text{SbSe}_{0.5}$  configurations. If  $y = 24$  and  $z = 16$  (from XPS fit), we need in total 32 Se atoms, while we have  $\sim 34$  available as estimated from (3). So, such scenario is theoretically possible via disproportionality analysis, owing to realistic accuracy of real composition and fit.

Here we have considered only 2 boundary compositions as an example, but similar arguments can be used to verify reliability of peak assignments for the remaining glass

compositions. Thus, on the basis of XPS and disproportionality analysis we conclude that covalent network of the investigated Ga-Sb-Se glasses should be preferentially built of  $[\text{GaSe}_{4/2}]$  tetrahedra, linked through Se atoms or Se-Se bridges with  $[\text{SbSe}_{3/2}]$  pyramids, where one or more of Se atoms are substituted with Sb in Se deficient compositions. Minor contributions to the network appear to be associated with Se-Se-Se chains,  $[\text{GaSe}_{3/2}]$  units and metal clusters.

#### **4. Conclusions**

Features in the valence band XPS spectra of the investigated Ga-Sb-Se glasses can be explained well by contribution of  $4p$  and  $4s$  electrons of Se,  $5p$  and  $5s$  electrons of Sb, as well as  $4s$  electrons of Ga. From the analysis of Ga, Sb and Se core level XPS spectra, we conclude that all glasses with 65 and 68 at.% of Se contain Se-Se-Se fragments in the concentration not exceeding 10 % of all Se sites. The samples with smaller Se content do not have these fragments in their network, but they still contain a significant concentration of Se-Se bonds. Majority of Ga atoms form 4-fold coordinated units, having Se as preferred neighbor. For some compositions the existence of 3-fold coordinated  $[\text{GaSe}_{3/2}]$  units, Ga-metal-bonded units, or Ga clusters of non-dissolved Ga are indicated on the basis of Ga  $3d$  XPS spectra analysis. Decrease in Se content causes partial or full destruction of  $[\text{SbSe}_{3/2}]$  pyramids by the replacement of one or more Se atoms with Sb or Ga metals.

#### **Acknowledgments**

The group from Austin Peay State University acknowledges financial support from NSF Grant DMR-1409160 and TN Spacegrant Consortium. The authors from University of Rennes-1 would like to acknowledge the IUF (Institut Universitaire de France).

#### **Conflict of Interest**

The authors declare no conflict of interest.

## References

- [1] D. Tonchev, S. O. Kasap, *J. Non-Cryst. Solids* **1999**, 248, 28.
- [2] J. S. Berkes, B. Myers, *J. Electrochem. Soc.: Solid State Sci.* **1971**, 118, 1485.
- [3] V. Damodara Das, K. S. Raju, S. Aruna, *J. Appl. Phys.* **1995**, 78, 1751.
- [4] M. Fadel, M. M. El-Samanoundy, K. A. Sharaf, *J. Mater. Sci.* **1995**, 30, 2377.
- [5] H. Sakata, N. Nakao, *J. Non-Cryst. Solids* **1993**, 163, 236.
- [6] Z. Sary, R. Novotny, J. Horak, J. Navratil, *J. Mater. Sci. Lett.* **1993**, 12, 359.
- [7] L. R. Gilbert, B. Vanpelt, C. Wood, *J. Phys. Chem. Solids* **1974**, 35, 1629.
- [8] K. A. Alzewel, H. H. Abou Sekkina, Z. M. Hanafi, *J. Phys. Chem.* **1975**, 94, 291.
- [9] A. Kaspus, J. Klapatauskas, *Leit Fiz. Rinkiny* **1974**, 14, 305.
- [10] A. Feltz, *Amorphous Inorganic Materials and Glasses*, VCH, Weinheim, **1993**.
- [11] Z. U. Borisova. *Glassy semiconductors*, Plenum Press, New York and London, **1981**.
- [12] M. Popescu. *Non-crystalline chalcogenides*, Kluwer Academic Publishers, New York, **2002**.
- [13] A. Lecomte, V. Nazabal, D. Le Coq, L. Calvez, *J. Non-Cryst. Solids* **2018**, 481, 543.
- [14] Y. Lu, S. Song, Y. Gong, Zh. Song, F. Rao, L. Wu, B. Liu, D. Yao, *Appl. Phys. Lett.* **2011**, 99, 243111.
- [15] Zh. Yang, W. Chen, L. Luo, *J. Non-Cryst. Solids* **2005**, 351, 2513.
- [16] J-L. Adam and X. Zhang (Ed.), *Chalcogenide Glasses: Preparation, Properties and Application*, Woodhead Publishing series in Electronic and Optical Materials No.44, **2014**.
- [17] R. Golovchak, A. Kovalskiy, A. C. Miller, H. Jain, O. Shpotyuk, *Phys. Rev. B* **2007**, 76, 125208.
- [18] R. Golovchak, O. Shpotyuk, S. Kozyukhin, A. Kovalskiy, A. C. Miller, H. Jain, *J. Appl. Physics* **2009**, 105, 103704.

- [19] R. Golovchak, O. Shpotyuk, J. S. McCloy, B. J. Riley, C. F. Windisch, S. K. Sundaram, A. Kovalskiy, H. Jain, *Phil. Magazine* **2010**, 90, 4489.
- [20] R. Golovchak, O. Shpotyuk, S. Kozyukhin, M. Shpotyuk, A. Kovalskiy, H. Jain, *J. Non-Cryst. Solids* **2011**, 357, 1797.
- [21] R. Golovchak, O. Shpotyuk, M. Iovu, A. Kovalskiy, H. Jain, *J. Non-Cryst. Solids* **2011**, 357, 3454.
- [22] D. Sati, A. Kovalskiy, R. Golovchak, H. Jain, *J. Non-Cryst. Solids* **2012**, 358, 163.
- [23] R. Golovchak, L. Calvez, E. Petracovschi, B. Bureau, D. Savitskii, H. Jain, *Materials Chem. & Physics* **2013**, 138, 909.
- [24] R. Golovchak, V. Nazabal, B. Bureau, J. Oelgoetz, A. Kovalskiy, H. Jain, *J. Non-Cryst. Solids* **2018**, 499, 237.
- [25] J. F. Moulder, W. F. Stickle, P. E. Sobol, K. D. Bomben, *Handbook of X-ray Photoelectron Spectroscopy* / Ed. J. Chastein. Perkin-Elmer Corp., Phys. Electr. Div., Eden Prairie, Minnesota, **1992**.
- [26] J. D. Conny, C. J. Powell, *Surf. Interface Anal.* **2000**, 29, 856.
- [27] I. Lefebvre-Devos, M. Lassalle, X. Wallart, J. Olivier-Fourcade, L. Monconduit, J. C. Jumas, *Phys. Rev. B* **2001**, 63, 125110.
- [28] J. M. Holender, M. J. Gillan, *Phys. Rev. B* **1996**, 53, 4399.
- [29] E. Bergignat, G. Hollinger, H. Chermette, P. Pertosa, D. Lohez, M. Lannoo, M. Bensoussan, *Phys. Rev. B* **1988**, 37, 4506.
- [30] A. Kovalskiy, H. Jain, A. Miller, R. Golovchak, O. Shpotyuk, *J. Phys, Chem. B* **2006**, 110, 22930.
- [31] L. Pauling, *The Nature of the Chemical Bond*, Cornell Univ. Press, Ithaca, **1960**.
- [32] J. H. Song, Y.G. Choi, J. Heo, *J. Non-Cryst. Solids* **2006**, 352, 423.
- [33] S. Tanabe, *J. Non-Cryst. Solids* **1999**, 259, 1.

- [34] E. Furet, A. Lecomte, D. Le Coq, F. Zeng, L. Cormier, C. Roiland, L. Calvez, *J. Non-Cryst. Solids* **2021**, 557, 120574.
- [35] H. Iwakuro, C. Tatsuyama, S. Ichimura, *Jpn. J. Appl. Phys.* **1982**, 21, 94.
- [36] E. Baudet, C. Cardinaud, A. Girard, E. Rinnert, K. Michel, B. Bureau, V. Nazabal, *J. Non-Cryst. Solids* **2016**, 444, 64.

**Table 1.** Best fit values ( $d_{5/2}$  components) of  $BE$  (eV),  $fwhm$  (eV) and  $A$  (%) parameters obtained from the fitting of Se 3d core level peaks (the analyzed element in structural fragments is in bold font).

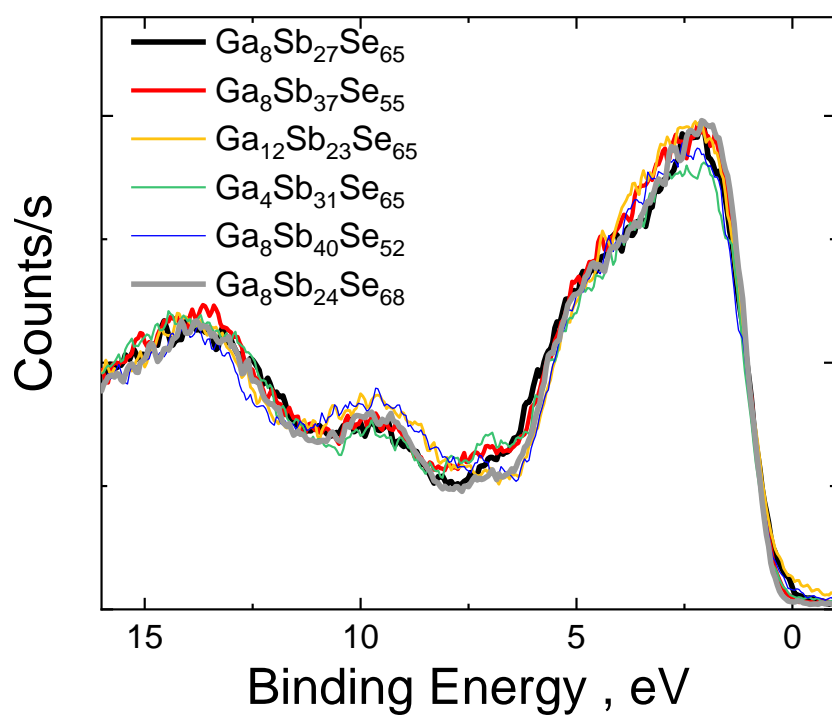
| Composition<br>/fragment                           | Se- <b>Se</b> -Se |        |     | Se- <b>Se</b> -(Sb,Ga) or Se <sub>2</sub> |        |     | Sb- <b>Se</b> -(Sb,Ga) |        |     | Ga- <b>Se</b> -Ga |        |     |
|--|-------------------|--------|-----|---|--------|-----|------------------------|--------|-----|-------------------|--------|-----|
|  | $BE$              | $fwhm$ | $A$ | $BE$                                      | $fwhm$ | $A$ | $BE$                   | $fwhm$ | $A$ | $BE$              | $fwhm$ | $A$ |
| Ga <sub>8</sub> Sb <sub>24</sub> Se <sub>68</sub>  | 54.74             | 0.70   | 8   | 54.15                                     | 0.86   | 32  | 53.72                  | 0.83   | 60  |                   |        |     |
| Ga <sub>4</sub> Sb <sub>31</sub> Se <sub>65</sub>  | 54.70             | 0.70   | 8   | 54.17                                     | 0.84   | 36  | 53.58                  | 0.85   | 49  | 53.15             | 0.81   | 7   |
| Ga <sub>8</sub> Sb <sub>27</sub> Se <sub>65</sub>  | 54.81             | 0.70   | 9   | 54.25                                     | 0.85   | 25  | 53.60                  | 0.88   | 56  | 53.15             | 0.83   | 10  |
| Ga <sub>12</sub> Sb <sub>23</sub> Se <sub>65</sub> | 54.83             | 0.62   | 2   | 54.17                                     | 0.86   | 21  | 53.62                  | 0.80   | 61  | 53.24             | 0.83   | 17  |
| Ga <sub>8</sub> Sb <sub>37</sub> Se <sub>55</sub>  |                   |        |     | 54.37                                     | 0.95   | 18  | 53.67                  | 0.95   | 64  | 53.22             | 0.86   | 18  |
| Ga <sub>8</sub> Sb <sub>40</sub> Se <sub>52</sub>  |                   |        |     | 54.45                                     | 0.95   | 7   | 53.68                  | 0.85   | 93  |                   |        |     |

**Table 2.** Best fit values ( $d_{5/2}$  components) of  $BE$  (eV),  $fwhm$  (eV) and  $A$  (%) parameters obtained from the fitting of Ga  $3d$  core level peaks (the analyzed element in structural fragments is in bold font).

| Composition<br>/fragment                           | (Se) <sub>2</sub> > <b>Ga</b> <(Se) <sub>2</sub> |        |     | (Se) <sub>3</sub> ≡ <b>Ga</b> -(Ga,Sb)<br>or (Se) <sub>2</sub> = <b>Ga</b> -Se |        |     |
|--|--|--------|-----|--|--------|-----|
|  | $BE$   | $fwhm$ | $A$ | $BE$   | $fwhm$ | $A$ |
| Ga <sub>8</sub> Sb <sub>24</sub> Se <sub>68</sub>  | 19.40  | 0.79   | 100 |  |        |     |
| Ga <sub>4</sub> Sb <sub>31</sub> Se <sub>65</sub>  | 19.40  | 0.92   | 100 |  |        |     |
| Ga <sub>8</sub> Sb <sub>27</sub> Se <sub>65</sub>  | 19.32  | 0.86   | 81  | 18.81  | 0.96   | 19  |
| Ga <sub>12</sub> Sb <sub>23</sub> Se <sub>65</sub> | 19.41  | 0.90   | 89  | 18.84  | 0.85   | 11  |
| Ga <sub>8</sub> Sb <sub>37</sub> Se <sub>55</sub>  | 19.31  | 0.93   | 96  |  |        |     |
| Ga <sub>8</sub> Sb <sub>40</sub> Se <sub>52</sub>  | 19.32  | 0.87   | 100 |  |        |     |

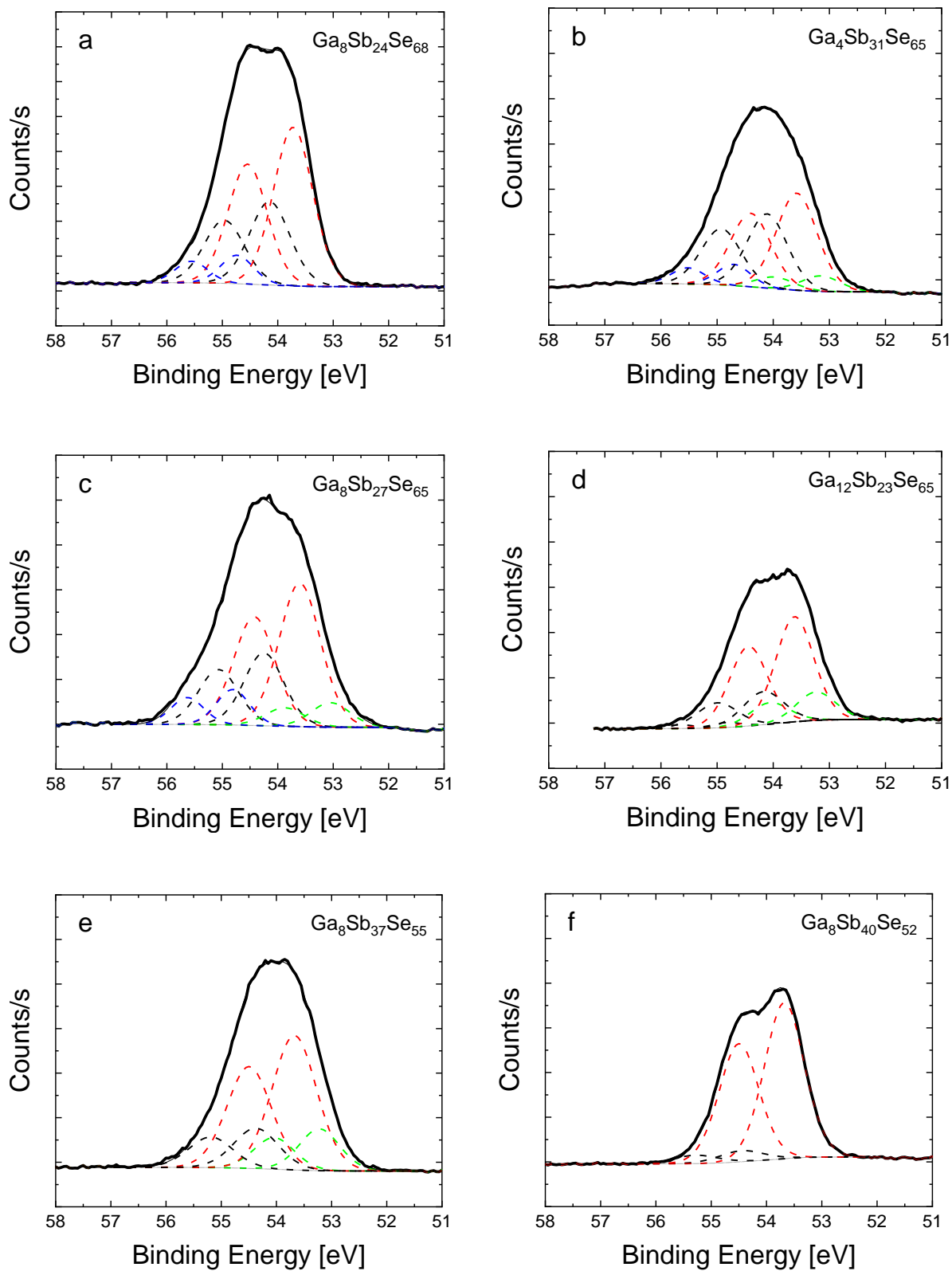
**Table 3.** Best fit values ( $d_{5/2}$  components) of  $BE$  (eV),  $fwhm$  (eV) and  $A$  (%) parameters obtained from the fitting of Sb  $4d$  core level peaks (the analyzed element in structural fragments is in bold font).

| Composition<br>/fragment                           | (Se) <sub>2</sub> > <b>Sb</b> -Se |        |     | (Se) <sub>2</sub> > <b>Sb</b> -(Ga,Sb) |        |     | (Sb) <sub>2</sub> > <b>Sb</b> -Se |        |     | (Sb) <sub>2</sub> > <b>Sb</b> -(Sb,Ga) |        |     |
|--|-----------------------------------|--------|-----|--|--------|-----|-----------------------------------|--------|-----|--|--------|-----|
|  | $BE$                              | $fwhm$ | $A$ | $BE$                                   | $fwhm$ | $A$ | $BE$                              | $fwhm$ | $A$ | $BE$                                   | $fwhm$ | $A$ |
| Ga <sub>8</sub> Sb <sub>24</sub> Se <sub>68</sub>  | 33.04                             | 0.77   | 100 |  |        |     |                                   |        |     |  |        |     |
| Ga <sub>4</sub> Sb <sub>31</sub> Se <sub>65</sub>  | 33.05                             | 0.82   | 50  | 32.57                                  | 0.82   | 50  |                                   |        |     |  |        |     |
| Ga <sub>8</sub> Sb <sub>27</sub> Se <sub>65</sub>  | 33.02                             | 0.86   | 59  | 32.70                                  | 0.82   | 37  |                                   |        |     | 31.87                                  | 0.75   | 4   |
| Ga <sub>12</sub> Sb <sub>23</sub> Se <sub>65</sub> | 33.03                             | 0.87   | 66  | 32.49                                  | 0.90   | 28  |                                   |        |     | 31.82                                  | 0.80   | 6   |
| Ga <sub>8</sub> Sb <sub>37</sub> Se <sub>55</sub>  |                                   |        |     | 32.73                                  | 0.89   | 95  | 32.10                             | 0.98   | 5   |  |        |     |
| Ga <sub>8</sub> Sb <sub>40</sub> Se <sub>52</sub>  |                                   |        |     | 32.74                                  | 0.87   | 60  | 32.08                             | 0.98   | 40  |  |        |     |

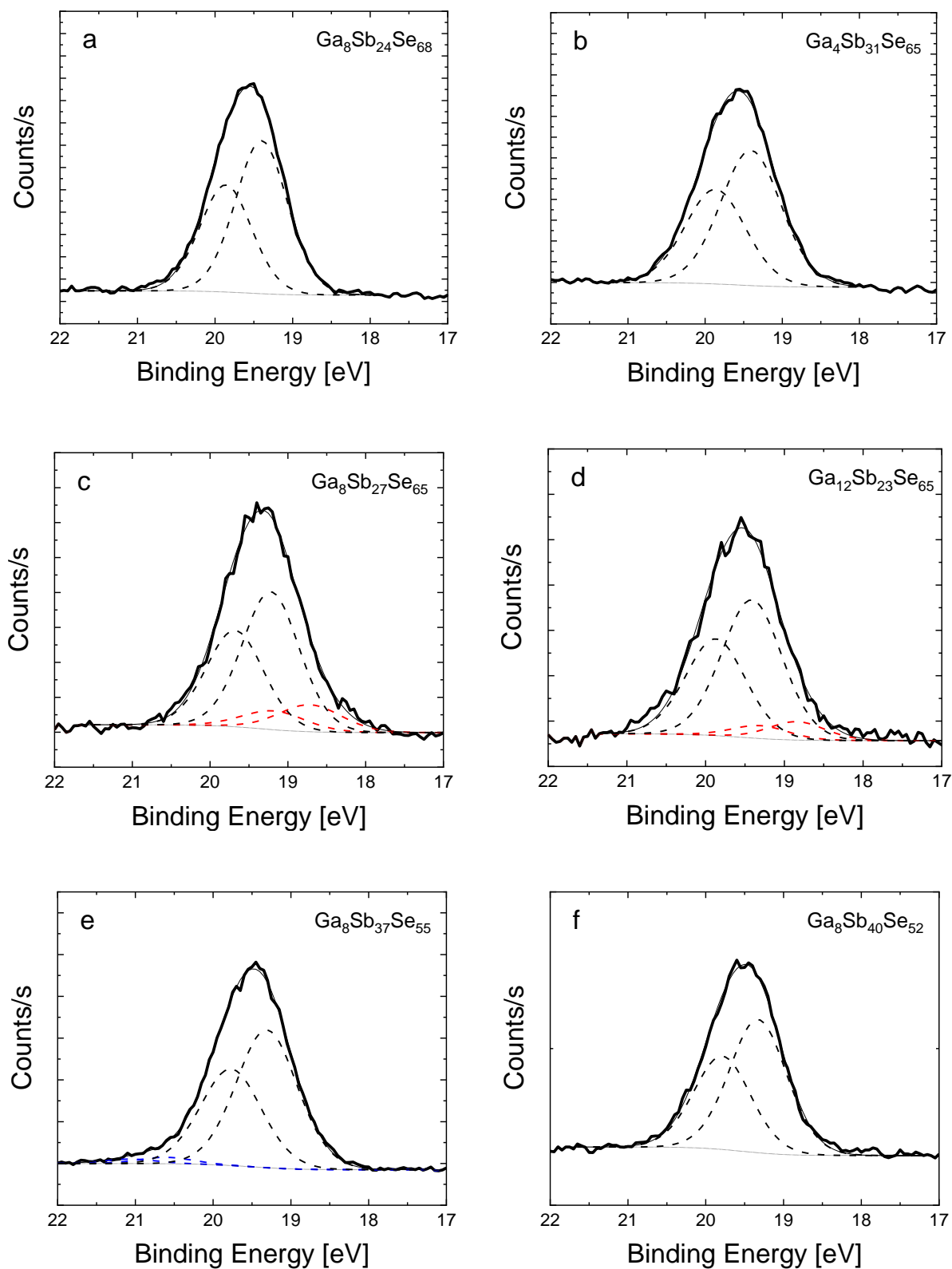


**Figure 1.** Valence band XPS spectra of the investigated Ga-Sb-Se glasses.

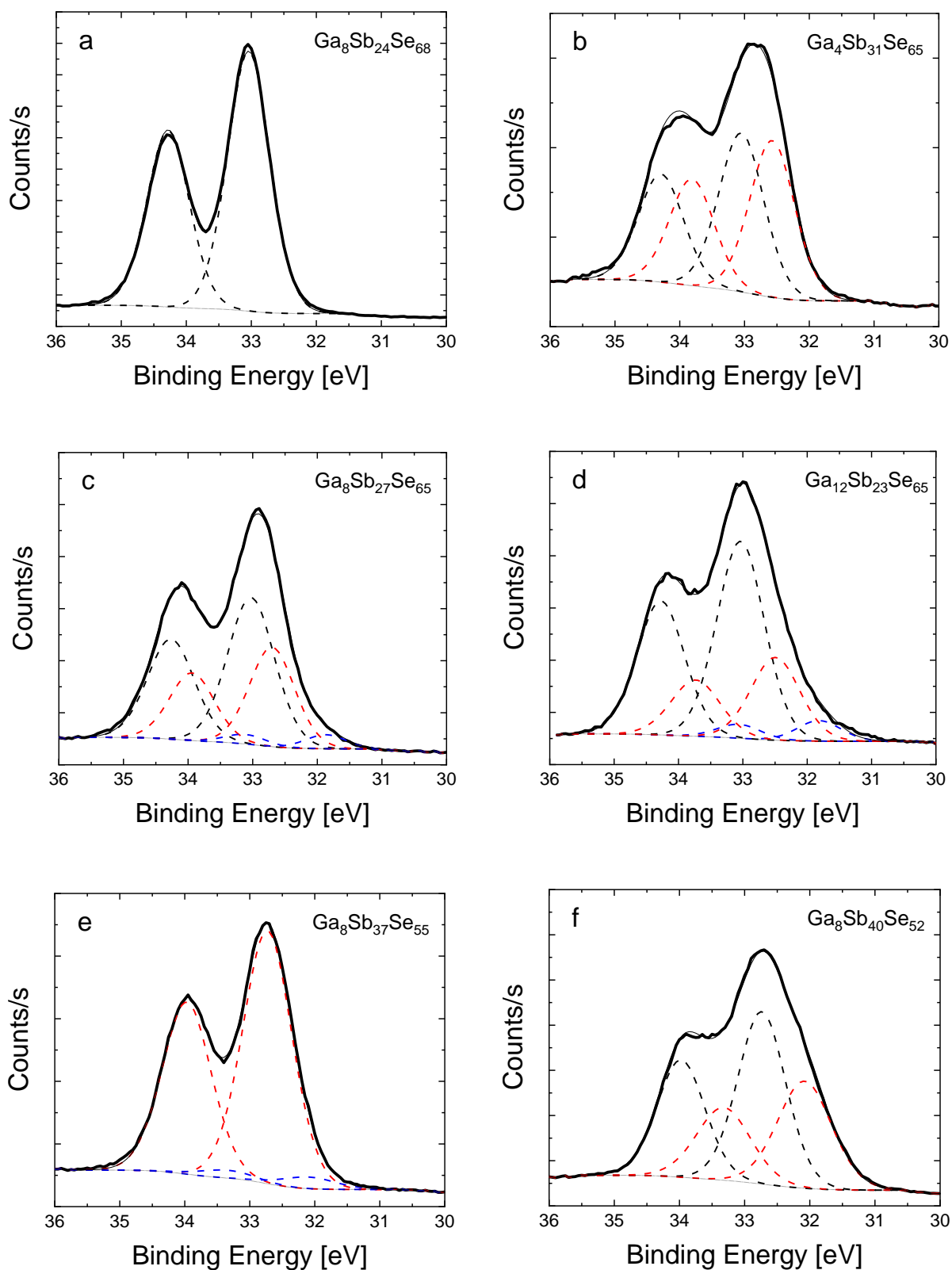




**Figure 2.** Experimental Se 3d core level XPS spectra (thick solid line), their fitting doublet components (dashed lines) and reconstructed from the fits theoretical curves (thin solid line) of the investigated Ga-Sb-Se glasses.



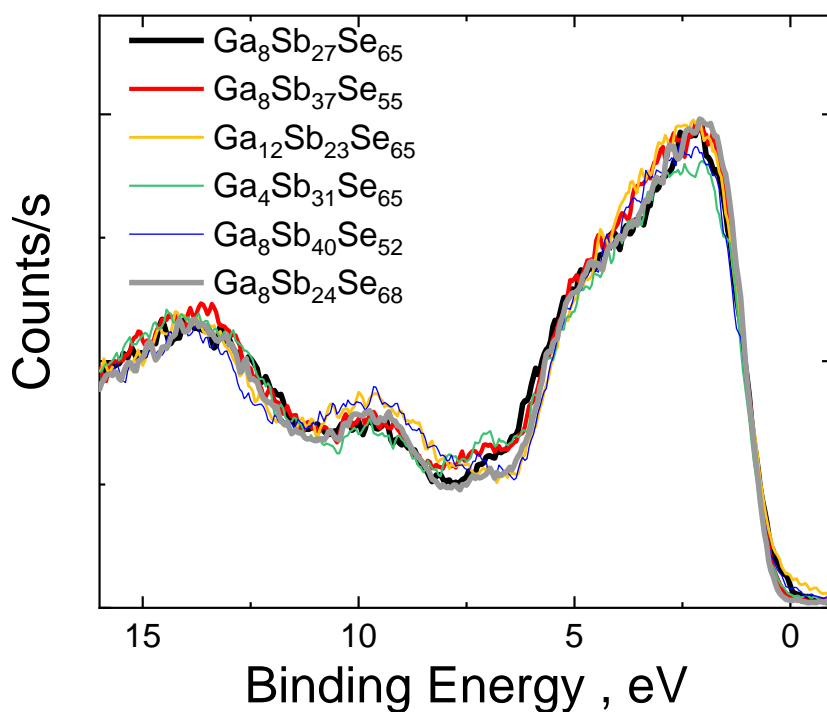
**Figure 3.** Experimental Ga 3d core level XPS spectra (thick solid line), their fitting doublet components (dashed lines) and reconstructed from the fits theoretical curves (thin solid line) of the investigated Ga-Sb-Se glasses.



**Figure 4.** Experimental Sb 4d core level XPS spectra (thick solid line), their fitting doublet components (dashed lines) and reconstructed from the fits theoretical curves (thin solid line) of the investigated Ga-Sb-Se glasses.

## Short abstract

The main structural building blocks of covalent Ga-Sb-Se glasses are revealed through the high-resolution core-level and valence band XPS spectra study. The results are supported by quantitative disproportionality analysis. The moieties of Se-Se-Se, Se-Se-(Ga/Sb) and (Ga/Sb-Se-Sb/Ga) fragments as well as Ga/Sb-based tetrahedral/pyramidal structural units are determined by fitting Se, Ga and Sb core-level spectra.



Valence band XPS spectra of the investigated Ga-Sb-Se glasses